The induction of macrophage hemeoxygenase-1 is protective during acute kidney injury in aging mice

David A. Ferenbach[1], Noemie C.J. Nkejabega[1,2], Jennifer McKay[1,2], Abhijeet K. Choudhary[1], Madeleine A. Vernon[1], Matthew F. Beesley[1], Spike Clay[1], Bryan C. Conway[1], Lorna P. Marson[1], David C. Kluth[1,2] and Jeremy Hughes[1,2]

[1]*MRC Centre for Inflammation Research, Queen's Medical Research Institute, University of Edinburgh, Edinburgh, UK*

Aging is thought to be associated with a higher susceptibility to renal ischemia–reperfusion injury (IRI). To study whether defective induction of hemeoxygenase-1 (HO-1, a protective and anti-inflammatory enzyme) might contribute to this, we found that while 12-month-old mice had similar baseline renal function and HO-1 expression, the induction of HO-1 usually seen in ischemia–reperfusion was reduced. This was also associated with worsened renal function and acute tubular necrosis in the aged compared with young mice. In the older mice, heme arginate (HA) induced HO-1 in the cortex and medulla, significantly improved renal function, and reduced tissue injury. Cellular HO-1 induction in the medulla in response to injury or HA treatment was found to be interstitial rather than epithelial, as evidenced by its colocalization with macrophage markers. *In vitro*, HA treatment of primary macrophages resulted in marked HO-1 induction without impairment of classical activation pathways. Macrophage depletion, caused by diphtheria toxin treatment of 12-month-old CD11b-DTR transgenic animals, resulted in the loss of interstitial HO-1-positive cells and reversal of the protective phenotype of HA treatment. Thus, failure of HO-1 induction following renal IRI worsens structural and functional injury in older mice and represents a therapeutic target in the elderly. Hence, HO-1-positive renal macrophages mediate HA-induced protection in IRI.

Kidney International (2011) **79,** 966–976; doi:10.1038/ki.2010.535; published online 19 January 2011

KEYWORDS: aged; cell ablation; hemeoxygenase; ischemia–reperfusion; macrophages

Correspondence: *David A. Ferenbach, MRC Centre for Inflammation Research, Queen's Medical Research Institute, University of Edinburgh, 47 Little France Crescent, Edinburgh EH16 4TJ, UK.*
E-mail: dferenbach@hotmail.com

[2]These authors contributed equally to this work.

Received 25 March 2010; revised 20 October 2010; accepted 16 November 2010; published online 19 January 2011

Acute kidney injury (AKI) is a devastating clinical condition with a high morbidity and mortality.[1] The elderly exhibit both markedly increased susceptibility to AKI,[2] and higher rates of death and progression to end-stage renal disease.[3,4] This heightened vulnerability to renal injury in the older population is conventionally thought to be multifactorial in etiology, with increased use of potentially nephrotoxic drugs superimposed on conditions such as arteriosclerosis resulting in an impaired ability to maintain adequate renal perfusion in response to other systemic insults.

It is recognized that in addition to the acquisition of comorbid conditions, aging also impacts on a cellular level as it may alter the ability of a tissue to respond to stress or to regenerate in response to injury.[5] A key enzyme induced by cell stress is hemeoxygenase-1 (HO-1), which catalyzes the breakdown of highly reactive free heme moieties. In addition to removing a source of oxidative stress, heme metabolism generates carbon monoxide and biliverdin that is subsequently converted to bilirubin by the enzyme biliverdin reductase. These products of heme metabolism exhibit immunomodulatory, antioxidant, antiapoptotic, and vasoactive properties.[6] HO-1 is induced in the kidney in response to ischemia–reperfusion injury (IRI),[7] and the administration of pharmacological inducers of HO-1 has been attempted with some success in renal IRI in young animals (reviewed by Nath[8]).

Expression of HO-1 in macrophages (Mϕ) opposes inflammatory activation and autoimmunity,[9,10] and is associated with improved outcome in both hepatic and renal IRI.[11,12] Recent studies have demonstrated that aged animals undergoing experimental hypoxic/hyperthermic brain injury, liver heat shock, or lung inflammation exhibit reduced ability to induce HO-1 compared with young control mice.[13–15]

This study sought to test the hypothesis that a failure of HO-1 induction in the aged kidney in response to IRI could contribute to the susceptibility to AKI seen in the aged population. Furthermore, the utility of the HO-1 inducer heme arginate (HA) was tested in an experimental model of AKI, and its cellular target of action investigated.

RESULTS

Young and 1-year-old mice have equivalent baseline renal function

Renal function was measured in young (6- to 8-week-old) and old (52- to 56-week-old) mice. Serum creatinine was not

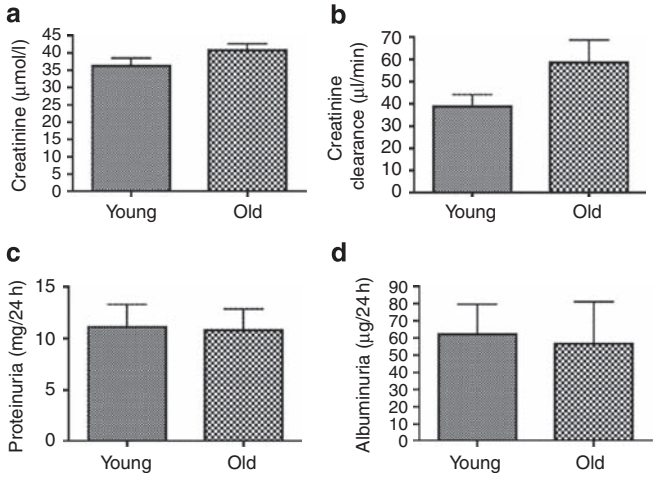

Figure 1 | Measurement of baseline renal function in old and young mice. Young and 1-year-old mice exhibit equivalent renal excretory function, with comparable serum creatinine (**a**, $n = 10$–11/group), measured 24-h creatinine clearance (**b**, $n = 5$/group), proteinuria (**c**, $n = 6$/group), and albuminuria (**d**, $n = 6$/group; all $P =$ not significant).

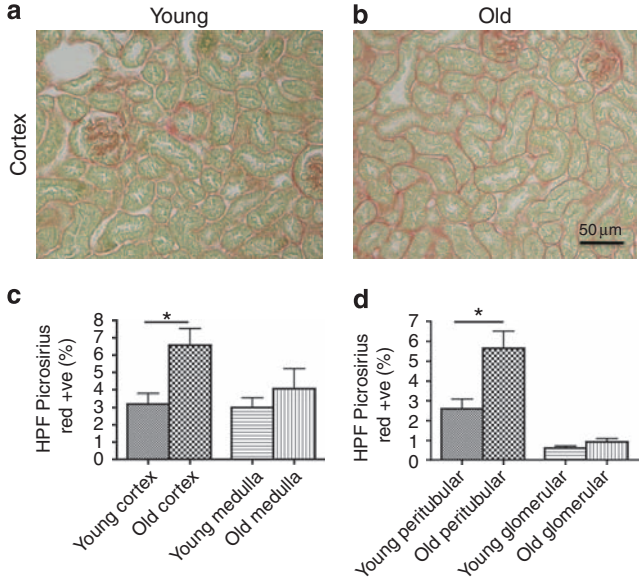

Figure 2 | Quantification of fibrillar collagen within old and young kidneys. Representative images of fibrillar collagen deposition shown by Picrosirius red staining (**a** and **b**, × 200 magnification). Image analysis demonstrates that old animals exhibit increased levels of fibrillary collagen deposition within the cortex compared with young controls (**c**; $*P = 0.018$ young vs old cortical Picrosirius red staining, $n = 5$/group). Further selective analysis of cortical images revealed that this excess was wholly due to peritubular rather than intraglomerular collagen accumulation (**d**; $P = 0.015$ young vs old peritubular staining). HPF, high power field.

significantly different between groups (Figure 1a, 36.6 ± 2.2 vs 40.8 ± 1.9 μmol/l; young vs old mice; $P =$ not significant (NS)). Further studies were undertaken using metabolic cage collections, demonstrating that older animals had normal 24-h creatinine clearance (Figure 1b, 39 ± 5 vs 58 ± 11 μl/min; young vs old mice; $P =$ NS) and urinary excretion of both total protein (Figure 1c, 11.1 ± 2.2 vs 10.8 ± 2.1 mg/24 h; young vs old mice; $P =$ NS) and albumin (Figure 1d, 62.3 ± 17.4 vs 56.7 ± 24.2 μg/24 h; young vs old mice; $P =$ NS). Assessment of fibrillar collagen deposition with Picrosirius red (Figure 2a and b) demonstrated equivalent collagen matrix within the medulla (Figure 2c), but increased levels of peritubular collagen deposition within the cortex of older animals (Figure 2d, 2.6 ± 0.5 vs $5.7 \pm 0.9\%$ of field Picrosirius red + ve; young vs old mice; $P = 0.015$).

Baseline immunohistochemistry was undertaken to examine the density of the microvasculature by CD31 staining in both cortex and medulla, which was found to be well maintained in old animals (Supplementary Figure S1 online). Baseline levels of intrarenal Mϕ, T and B lymphocytes, and neutrophils were all determined by immunohistochemistry (Supplementary Figure S2A online), with no difference in counts between young and older mice (Supplementary Figure S2B online).

One-year-old mice exhibit increased renal injury following renal IRI

To characterize whether 1-year-old mice exhibited an increased susceptibility to AKI, despite normal basal excretory function, young and 1-year-old mice underwent 20 min of experimental IRI with contralateral nephrectomy; a model that causes only mild renal dysfunction in young female animals, peaking at 24 h post-injury. At 24 h post-injury, older animals exhibited marked acute renal failure (Figure 3a, creatinine 38 ± 6 vs 120 ± 35 μmol/l; young vs 1-year–old mice; $P < 0.01$), with increased levels of acute tubular necrosis (ATN; Figure 3B, images Figure 3d–g, 55 ± 0.4 vs $75 \pm 1.2\%$ ATN; young vs 1-year-old mice; $P < 0.001$). There was significant recruitment of neutrophils on day 1 in older mice (Figure 3c, 0.4 ± 0.1 vs 22.5 ± 7.3 neutrophils/high power field, $P = 0.0032$) with less neutrophil infiltration evident in the young animals. There was no significant difference in the numbers of Mϕ, T or B cells between groups at 24 h (Supplementary Table S1 online).

Older mice fail to upregulate HO-1 protein in the outer medulla in response to renal IRI

Baseline HO-1 levels were assessed in both cortex and medulla by immunohistochemistry and image analysis, which demonstrated low levels of basal tubular HO-1 expression in both the young and 1-year-old kidney (Figure 4a–c and e). The ability of the aged animal kidney to induce HO-1 in response to IRI was assessed by immunohistochemistry to permit spatial localization of protein (Figure 4c–f). Within the cortex, both young and older animals induced HO-1 in response to IRI (Figure 4a), although this induction was blunted in the aged group. In contrast to young mice, aged animals exhibited significantly less induction of HO-1 within the medulla in response to IRI (Figure 4b, $P = 0.0013$). Although young mice exhibited nearly twofold greater number of viable medullary tubules after IRI (44.8 vs 24.5%; young vs year old mice), the greater than fivefold increase in medullary HO-1 expression in the medulla of young compared with aged mice indicated that the increased

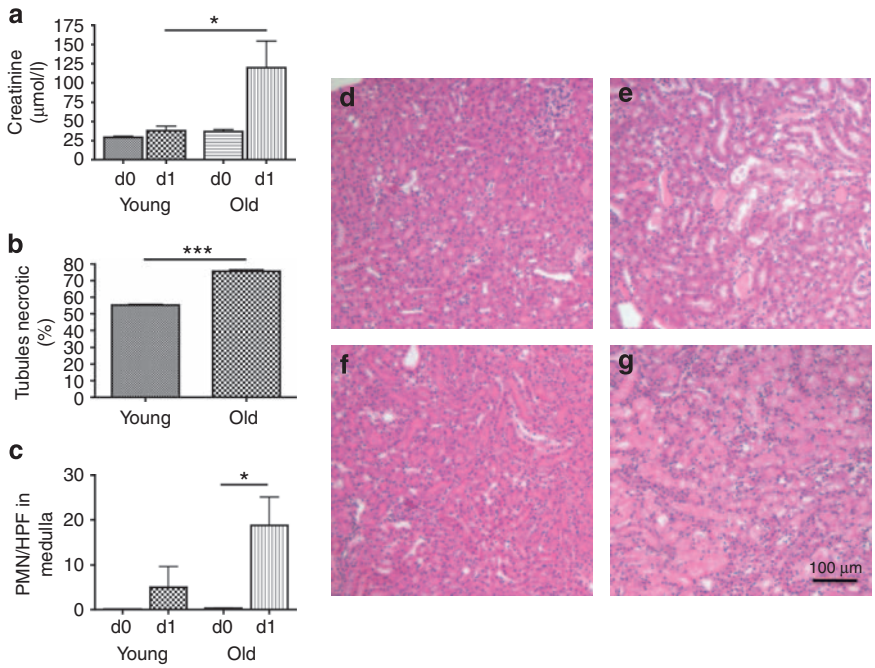

Figure 3 | Outcome after renal ischemia-reperfusion injury in young and old mice. Old mice demonstrate worse functional derangement after ischemia–reperfusion injury (IRI; **a**; $^{*}P = 0.016$, $n = 5$/group), with associated increased levels of acute tubular necrosis (**b**; $^{***}P < 0.0001$). The increased injury in old mice was associated with increased recruitment of neutrophils from baseline (**c**; $^{*}P = 0.0032$). Hematoxylin and eosin images of young kidney pre-IRI (**d**) and post-IRI (**e**), and old kidney pre-IRI (**f**) and post-IRI (**g**) (all images $\times 100$). PMN, polymorphonuclear neutrophil; HPF, high power field.

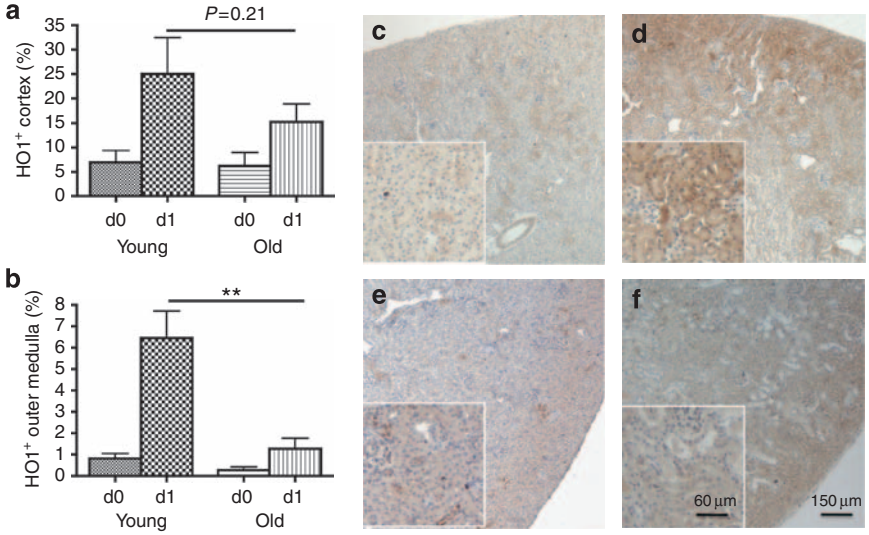

Figure 4 | Renal hemeoxygenase-1 expression after IRI in young and old kidneys. Hemeoxygenase-1 (HO-1) protein is induced in the cortex of old and young mice in response to ischemia–reperfusion injury (IRI; **a**, $P = 0.21$ young d1 vs old d1, $n = 4$–7/group), while there is a failure to induce HO-1 in the medulla of old mice (**b**, $^{**}P = 0.0013$ young d1 vs old d1, $n = 4$–7/group). Immunohistochemistry of HO-1 protein distribution in young animal kidney pre-IRI (**c**) and post-IRI (**d**), and old kidney pre-IRI (**e**) and post-IRI (**f**) (main images $\times 50$, insets $\times 125$).

induction was not simply an artifact of increased tubular viability.

Treatment of aged mice with HA results in renal HO-1 induction

To probe whether the failure to induce HO-1 was of functional significance in old mice, the HO-1-inducing agent HA was administered to 1-year-old mice 24 h before IRI. Western blots for HO-1 were performed on whole kidney homogenate (Figure 5a), and densitometric analysis was performed showing robust protein induction (Figure 5b; $P < 0.0005$, phosphate-buffered saline (PBS) vs HA). Immunohistochemical staining for HO-1 demonstrated induction in cortical tubules in HA pretreated animals (Figure 5d vs PBS control Figure 5c), resulting in markedly increased total cortical staining, which was maintained in the aftermath

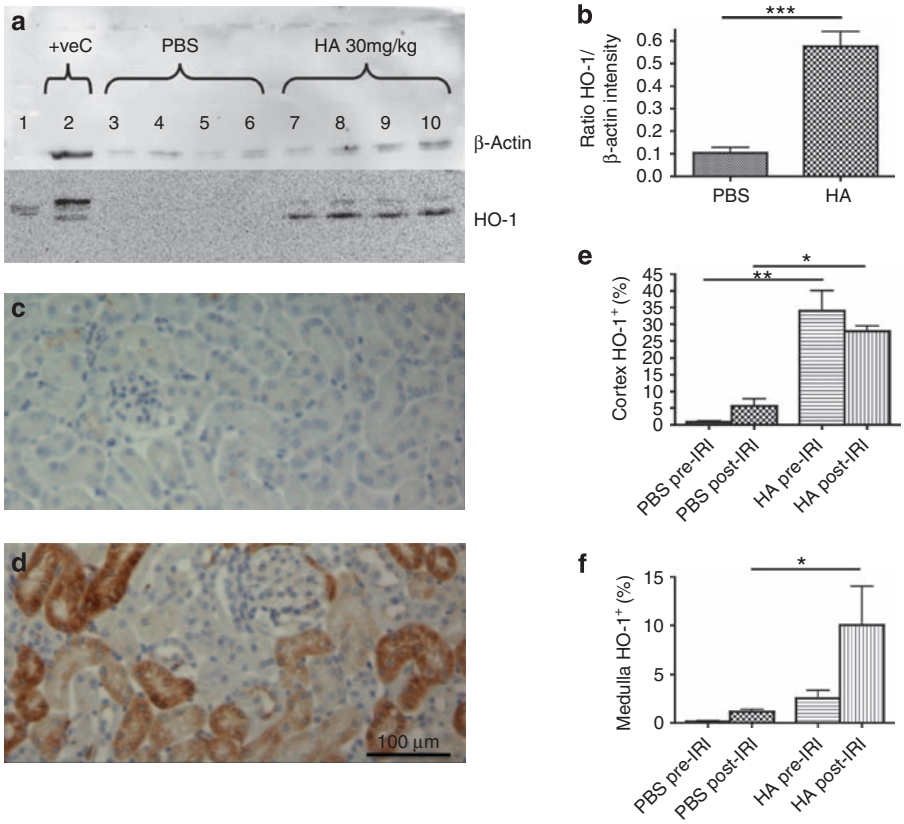

Figure 5 | Effects of heme arginate administration on renal hemeoxygenase-1 expression. Pretreatment with heme arginate (HA) at a dose of 30 mg/kg results in the induction of total kidney hemeoxygenase-1 (HO-1) protein by western blotting (**a**, positive control of liver homogenate: lane 2, vehicle-treated kidney: lanes 3–6, HA-treated kidney: lanes 7–10), and subsequent densitometric analysis (**b**, ***$P<0.001$). HO-1 expression in the cortex of old mice was minimal following phosphate-buffered saline (PBS) injection (**c**). HO-1 expression was markedly induced in the uninjured cortex following injection of HA (**d**). Image analysis demonstrated increased cortical HO-1 expression (**e**, **$P<0.001$ HA pre-ischemia–reperfusion injury (IRI) vs PBS pre-IRI; *$P<0.01$ HA post-IRI vs PBS post-IRI; $n=5$/group) and increased medullary HO-1 (**f**, *$P<0.05$ HA post-IRI vs PBS post-IRI; $n=5$/group) expression following HA treatment.

of IRI (Figure 5e, $P<0.001$ vs PBS treatment d0, $P<0.01$ vs PBS treatment d1). HA pretreatment increased HO-1 staining within the medulla with a further increase evident after IRI relative to PBS control (Figure 5f, $P<0.05$ d1 vs PBS treatment).

The effect of HA administration on circulating leukocyte number was assessed by flow cytometry. HA administration did not result in a significant change in total leukocyte number compared with sham injection (5.9 ± 1.2 vs $4.1 \pm 0.3 \times 10^6$ cells/ml whole blood, HA vs PBS; $P=0.21$, Supplementary Figure S3A online). Further analysis demonstrated that HA treatment was associated with an increase in circulating neutrophil counts and a decrease in Gr1+ monocytes (both $P=0.03$ vs pretreatment counts, summarized in Supplementary Figure S3B–F online).

Heme arginate pretreatment of aged mice ameliorates renal failure and tissue injury after IRI

To assess the potential for HO-1 induction as a therapeutic intervention in aged animals, renal IRI was performed in old animals 24 h after either intravenous injection of PBS (old + PBS) or HA (old + HA), with further young animals as controls (young + PBS). HA therapy was associated with marked functional protection (Figure 6a: creatinine 128.5 ± 31.5 vs 49.6 ± 6.3 vs 68.0 ± 10.0 μmol/l; old + PBS vs old + HA vs young + PBS; $P<0.05$). This was associated with a marked reduction in the severity of ATN in HA pretreated animals (Figure 6b–f: 58.4 ± 12.9 vs 21.0 ± 6.5 % ATN; old + PBS vs old + HA; $P<0.05$).

Heme arginate treatment induces HO-1 expression in interstitial cells of the kidney

In PBS-treated older animals, there were virtually no HO-1$^+$ interstitial cells evident at baseline (Figure 7a), but HO-1$^+$ interstitial cells were evident within injured areas after IRI (Figure 7b). Furthermore, after HA treatment, numerous interstitial cells were observed to express HO-1 (Figure 7c), and these HO-1$^+$ interstitial cells were present in maintained numbers after IRI (Figure 7d and e). Indeed, these HO-1$^+$ interstitial cells formed the principal site of HO-1 expression within the injured medulla (Figure 7b). Given the morphological and anatomical resemblance of these HO-1$^+$

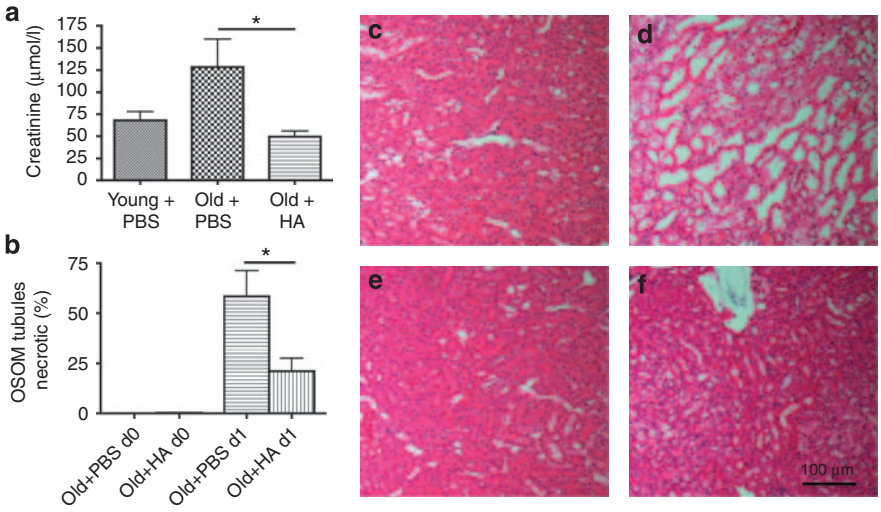

Figure 6 | Effect of heme arginate administration on renal injury and function after IRI in old animals. Heme arginate (HA) pretreatment of aged mice results in significant functional protection from ischemia–reperfusion injury (IRI) compared with vehicle-treated controls (**a**; $*P<0.05$; old + phosphate-buffered saline (PBS) vs old + HA, $n=5$–7/group). There was an associated reduction in the extent of acute tubular necrosis between groups (**b**; $*P<0.05$; old + PBS vs old + HA). Representative images demonstrate renal histology in PBS-treated mice pre-injury (**c**), PBS post-injury (**d**), HA-treated mice pre-injury (**e**), and HA post-injury (**f**) (all images × 200 magnification). OSOM, outer stripe of the outer medulla.

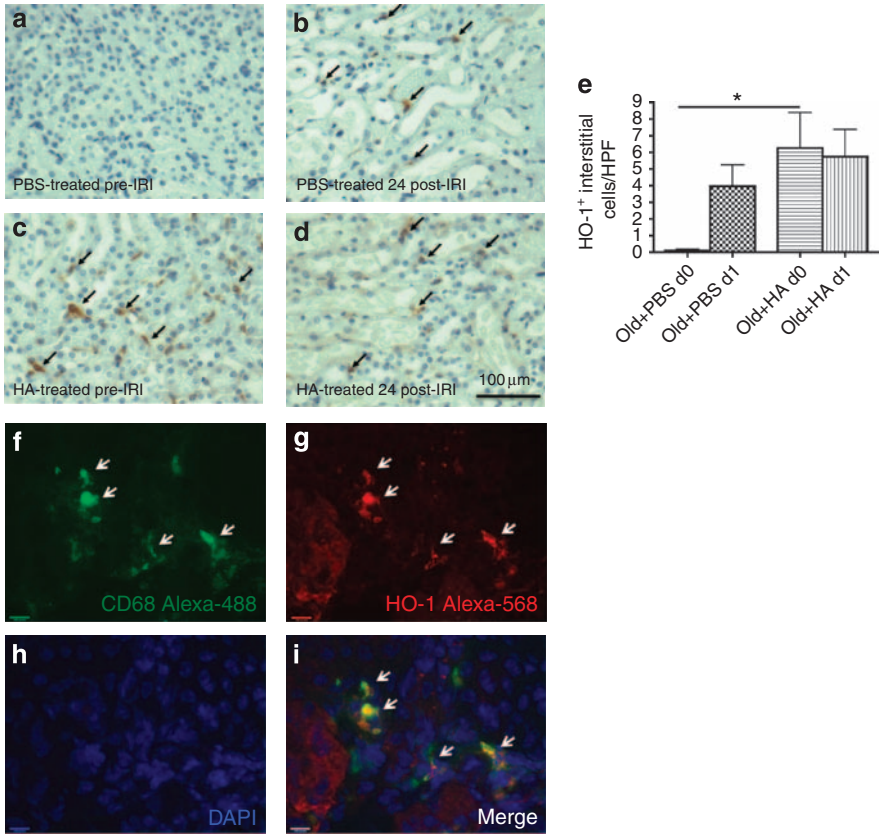

Figure 7 | Characterization of hemeoxygenase-1 expressing cells in the renal interstitium. Hemeoxygenase (HO)-1^+ interstitial cells are not present at baseline in old mice (**a**) but are evident following ischemia–reperfusion injury (IRI; **b**). Heme arginate (HA) administration results in an increased number of cells within the interstitial compartment of the outer medulla, which are strongly positive for HO-1 both pre- and post-IRI (**c**, pre-IRI **d**, post-IRI, **e**, mean HO-1^+ cell per high powered medullary field (HPF); $*P<0.05$ HA d0 vs phosphate-buffered saline (PBS) d0, $n=5$/group). Immunofluorescence of frozen sections for CD68 Alexa-488 (**f**), HO-1 Alexa-568 (**g**), and 4,6-diamidino-2-phenylindole (DAPI) (**h**) demonstrates multiple areas of colocalization (**i**), dual-positive cells marked with arrows) indicating that macrophages express HO-1 in the kidney in response to IRI or HA treatment.

interstitial cells to renal Mϕ, dual immunostaining with the resident Mϕ/dendritic cell marker CD68 was performed, demonstrating multiple areas of colocalization (Figure 7f–i), thereby indicating that one target of HA action is the resident mononuclear phagocyte population of the kidney.

Heme arginate treatment induces HO-1 in primary bone marrow-derived macrophages *in vitro*

To further demonstrate the ability of HA to upregulate Mϕ HO-1 expression, studies were undertaken in primary cultures of murine bone marrow-derived Mϕ (BMDM). Twenty-four hours treatment of Mϕ with HA (10 μmol/l) significantly increased HO-1 protein expression by western blot (Supplementary Figure S4A online) and immunofluorescence (Supplementary Figure S4B–E online). Increased HO-1 protein expression persisted for 24 h, following removal of HA containing media from the Mϕ.

The effect of HA treatment on resting and classically activated Mϕ phenotype was tested by stimulation with lipopolysaccharide and interferon-γ after preincubation with a range of HA doses. HA treatment *per se* had no activating effect on Mϕ (Supplementary Figure S4F online). Importantly, the cells also had preserved and unaltered ability to upregulate tumor necrosis factor-α in response to classical activating stimuli (Supplementary Figure S4F online, $P = \text{NS}$ by analysis of variance, $n = 3$/group).

Macrophage depletion results in loss of HA-induced renal protection

Our data indicated that interstitial cells, including Mϕ, represented an important site of HO-1 induction within the medulla of HA pretreated mice, and are either induced or recruited in PBS-treated animals in response to ischemic medullary injury. We therefore sought to probe the relative contribution of HO-1$^+$ interstitial Mϕ to the protected phenotype induced by treatment with HA. We used 1-year-old CD11b-DTR mice, in which Mϕ can be selectively depleted from the kidney by administration of diphtheria toxin (DT).[16,17] Aged CD11b-DTR mice were pretreated with either PBS, DT + PBS, HA + PBS, or HA + DT before undergoing renal IRI. Animals treated with DT exhibited a 75% reduction in resident F4/80$^+$ Mϕ counts (11.5 ± 2.3 vs 2.9 ± 0.7 F4/80+ cells/ × 400 field; PBS vs DT treatment; $P = 0.0024$).

In the cortex, where the predominant site of HO-1 induction was tubular, there was no difference in the level of HO-1 induction in day 0 nephrectomy specimens from DT-treated animals (Figure 8c). In contrast, DT pretreatment resulted in a five- to sixfold reduction in day 0 HO-1 staining in the medulla, where HO-1$^+$ interstitial cells represent the major site of HO-1 expression (Figure 8d, $P = 0.08$). HO-1$^+$ interstitial cells were then counted in the aftermath of IRI (Figure 8a and b), and were reduced by 60% in mice treated with HA + DT compared with mice treated with HA alone (Figure 8e: 4.2 ± 1.6 vs 10.4 ± 2.0 HO-1$^+$ interstitial cells/high power field; HA + DT vs HA + PBS; $P < 0.05$), indicating that CD11b$^+$ Mϕ represent the majority of HO-1$^+$ interstitial cells.

When functional outcome after IRI was assessed, HA + PBS-treated mice again demonstrated a markedly protected functional phenotype, which was abolished in HA + DT-treated mice (Figure 8f: creatinine 43.4 ± 3.3 vs 75.3 ± 11.6 vs 74.2 ± 11 vs 103.2 ± 22 μmol/l; HA + PBS vs HA + DT vs PBS vs DT + PBS; $P < 0.05$ HA + PBS vs HA + DT). Consistent with this, HA + PBS-treated animals demonstrated a significant reduction in the extent of acute tubular necrosis, which was not present in the context of concurrent Mϕ depletion (Figure 8g: ATN score 20 ± 8.1 vs 50.6 ± 7.3% vs 54 ± 10 vs 58.9 ± 10.1% outer stripe of the outer medulla necrosis; HA + PBS vs HA + DT vs PBS vs DT + PBS; $P < 0.05$ HA + PBS vs all groups).

DISCUSSION

These data demonstrate that while expressing comparable levels of baseline protein, the older animal kidney has an impaired ability to upregulate HO-1 in response to IRI, and demonstrates a worsened injury phenotype compared with young animals. HA administration to 1-year-old animals robustly induces HO-1 protein expression in both cortical tubules and interstitial medullary Mϕ, and provides aged mice with both structural and functional protection from IRI. This protected phenotype is absent in animals treated with HA coupled with conditional Mϕ ablation, strongly implicating the interstitial Mϕ as the key therapeutic target for HA.

Earlier work has described histological changes in kidneys of aged rats, with interstitial fibrosis, progressive tubular injury, glomerulosclerosis, and leukocyte recruitment.[18] While there was evidence of increased deposition of fibrillar collagen around the cortical tubules of aged animals, this was not associated with any capillary rarefaction or leukocyte infiltration. Such differences may reflect species and strain differences in the aging process, and also the earlier time point of 52–56 weeks chosen for the mouse studies presented here. Intriguingly, and in contrast to population studies in humans, studies of rats subjected to IRI after 5/6th nephrectomy, with resultant proteinuria and fibrosis, saw no increase in AKI severity,[19] thereby suggesting that reduced nephron number, fibrosis, and disruption of glomerular integrity are not absolute predictors of a worse outcome after IRI.

It is debatable to what 'human age' the mice examined in this study are equivalent. Laboratory mice in specific pathogen-free housing live considerably longer than their wild equivalents, with the 1-year-old time point studied here representing the average life expectancy for a wild mouse. While laboratory animals can live to twice this age, the majority of FVB strain mice have developed tumors by 24 months of age, confounding their experimental use.[20] Indeed preliminary studies were attempted in animals 18–20 months old, but were confounded by the high rates of malignancies discovered at laparotomy, and husbandry

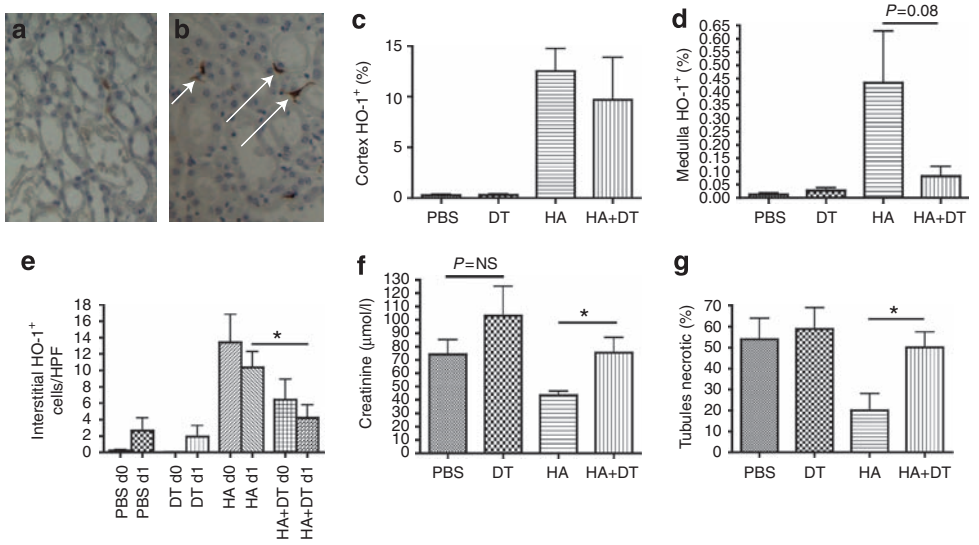

Figure 8 | Effects of macrophage depletion on heme arginate induced protection from IRI. Macrophage depletion of CD11b-DTR transgenic mice results in loss of the interstitial hemeoxygenase (HO)-1$^+$ cells induced by heme arginate (HA) treatment (**a**: HA treatment, **b**: HA treatment + Mϕ depletion, arrows indicate HO-1$^+$ cells). Image analysis demonstrates preserved cortical HO-1 induction (**c**), but a trend towards reduced medullary staining for HO-1 (**d**; $P = 0.08$ HA vs HA + diphtheria toxin (DT), $n = 5$/group). Quantification of interstitial HO-1$^+$ cells demonstrates a significant reduction in medullary interstitial HO-1$^+$ cells in HA + DT cotreated animals at d1 post-injury (**e**; *$P < 0.05$ HA vs HA + DT). The functional (**f**; *$P < 0.05$ HA vs HA + DT) and structural (**g**; *$P < 0.05$ HA vs HA + DT) protection of HA pretreatment is abolished in mice depleted of renal Mϕ. NS, not significant.

concerns regarding the relative frailty of the subjects before surgical intervention. Accordingly, the results as presented likely reflect the altered physiological response of subjects in the later third and fourth quartiles of pathogen-free population age.

It is well established from registry data that increasing age is a significant risk factor for AKI.[2] Similarly, there are precedents in rat models of renal IRI demonstrating that aged animals have a more marked reduction in the glomerular filtration rate associated with a marked increase in renal vasoconstriction.[21] Given the absence of either nephrotoxic drugs or indeed diverse intercurrent illnesses in the data presented here, such findings support the hypothesis that there are intrinsic alterations within the aged animal kidney that influence its response to a hypoperfusion insult. Given that pre-existing chronic renal failure is a major additional risk factor for AKI and subsequent end-stage renal failure in patients,[3] it was important to establish whether 'renal senescence' had led to a detectable sign of incipient renal impairment within the aged animals. The equivalence of measured creatinine clearance and albumin excretion rate demonstrated by the groups provided acceptable surrogates for the study of *de novo* AKI.

The finding of a reduced ability to upregulate HO-1 within the aged murine kidney echoes findings in other rodent models of inflammatory disease in bowel,[22] liver,[13] and brain.[14] These conserved effects across both species and organ systems would support this being a fundamental component of the aging process. The potential for HO-1 deficiency to impact on disease states is demonstrated by clinical data from renal transplantation, pulmonary emphysema, and atherosclerosis, where patients with transcription reducing polymorphisms in the human HO-1 gene have worsened disease phenotypes (reviewed by Exner *et al.*[23])

HO-1 is induced by a diverse range of noxious stimuli (reviewed by Wagener *et al.*[6]), but the mechanism by which HO-1 fails to respond to inducing stimuli in the aged remains incompletely characterized. The HO-1 inducing transcription factor *nrf2* represents a plausible target, being a key mediator of the IRI-mediated stress response such that genetic ablation of *nrf2* results in worsened severity of renal IRI.[24,25] *Nrf2* is also a pathway of pharmacological HO-1 induction,[26] and its basal levels have been shown to be suppressed in astrocytes of aged mice.[27] As such, this remains an area of ongoing investigation. Downstream of HO-1, both HA and hemin (a related HO-1 inducer) inhibit nuclear factor-κB;[28,29] a key pathway mediating classical Mϕ activation with nuclear factor-κB inhibition previously demonstrated to modulate experimental renal disease.[30] Given the vital role played by the Mϕ as an effector arm of the innate immune system, it is of note that the *in vitro* experiments demonstrated that HO-1 induction was achieved without blunting of the ability to adopt a classically activated phenotype. This is important if the therapeutic translation of these therapies into an elderly patient population is not to be curtailed by the threat of immunosuppression and infection.

It is known that IRI induces HO-1 mRNA, protein, and activity in young experimental animals.[7,31] Additionally, data from pre- and post-implantation biopsies of human renal allografts demonstrates that HO-1 induction is maximal in

organs subject to delayed graft function.[32] Although such tissue homogenate-based methods do not allow interrogation of the specific cellular sites of HO-1 induction, studies using hemin as an inducing agent have demonstrated induction of HO-1 in both tubular and peritubular cells by immunohistochemistry.[33,34] Our findings demonstrate that HO-1 induction occurs in both cortical tubules and within the interstitial cells of both cortex and medulla in response to IRI and HA administration. HO-1 induction in organ resident Mϕ has been demonstrated to be of benefit in hepatic IRI,[12] and is thought to represent a component of the beneficial effects of statins on various disease models including renal IRI.[11]

Despite widespread tubular induction of HO-1 protein being present in response to HA therapy, the protected phenotype associated with this therapy was abolished in animals subject to conditional Mϕ ablation. There is a published literature demonstrating that Mϕ depletion *per se* is not deleterious in renal IRI, and indeed systemic administration of clodronate liposomes leads to widespread Mϕ depletion in the liver, spleen, and kidneys and improved outcome in renal IRI.[35,36] Our findings demonstrate that HO-1$^+$ Mϕ are key contributors to mediating HA-induced protection following IRI. This would be consistent with previous work in the liver demonstrating that depletion of HO-1$^+$ Kupffer cells sensitized the liver parenchyma to subsequent IRI injury.[12] Although DT does not ablate major Mϕ pools within the liver and spleen, it remains possible that that extra-renal Mϕ populations contribute to the protective effects of HA.

The phenotype of Mϕ-ablated animals suggests that the induction of HO-1 within non-myeloid lineages both within the kidney and at extra-renal sites is dispensible for the generation of a protective phenotype. Similarly, the systemic release of HO-1 generated carbon monoxide leading to altered circulatory responses would not appear critical to organ protection, unless such a factor was being generated exclusively by a myeloid cell population that was effectively depleted by the administration of DT. Interestingly, although circulating neutrophil numbers were increased by HA treatment, infiltration into the tissue was reduced, augering against this being of pathogenic significance. HO-1$^+$ Mϕ appear to facilitate the survival of medullary tubules, a finding which echoes results from studies of the developing kidney in which the resident embryonic Mϕ population are trophic for tubular growth and survival.[37] The identity of the HO-1$^+$F4/80$^-$ cells also visible by immunofluorescence remains unresolved, but may reflect the heterogeneity of the marker profile of Mϕ/dendritic cells within the kidney,[38] where at least 28% of resident renal CD11b$^+$CX3CR1$^+$ mononuclear phagocytes are F4/80$^-$.[39]

The data set as presented demonstrate an association between the presence of HA-induced HO-1 expressing renal Mϕ and improved outcome after IRI. These studies do not allow conclusions to be drawn as to whether HO-1 itself directly mediates this reduction in injury severity or is acting as a marker of a beneficial Mϕ population. The ability to selectively inhibit Mϕ HO-1 in cell lineages would permit further dissection of the role of Mϕ HO-1 in disease evolution, and the recent generation of the HO-1^{M-KO} mice lacking HO-1 in myeloid cells[9] could facilitate experiments leading to definitive conclusions regarding the role of Mϕ HO-1 induction in mediating the phenotype presented here. HO-1^{M-KO} mice exhibit a pattern of augmented bacterial killing and worsened autoimmune phenotype consistent with HO-1 acting as a 'molecular brake' on Mϕ cytotoxicity.

Published work, consistent with the findings from the HO-1^{M-KO} mouse, suggests that overexpression of HO-1 in a model of shock liver results in an inhibition of inflammatory cytokine production with reduced tumor necrosis factor-α and augmented interleukin-10 release.[40] Our own recent work has demonstrated a similar pattern of tumor necrosis factor-α and interleukin-10 production in lipopolysaccharide/interferon-γ-stimulated primary murine macrophages following adenovirally mediated HO-1 overexpression.[41] In these experiments administration of HO-1 overexpressing Mϕ after IRI improved subsequent renal function.

Taken together, these findings demonstrate that HO-1$^+$ interstitial Mϕ are beneficial in renal IRI, with a failure in their generation associated with the increased susceptibility to IRI exhibited by aged animals. Furthermore, HA can potently induce these cells in aged mice and restore a protected phenotype. As HA is licenced for use in humans (as a treatment for porphyria), it has translatable potential as a novel therapeutic strategy for the prophylaxis of AKI in susceptible populations, such as the elderly undergoing major surgery or on admission to critical care environments.

MATERIALS AND METHODS

Materials and reagents

Tissue culture reagents were purchased from Life Technologies (Paisley, UK). Tissue culture plastics were obtained from Costar (Loughborough, Leicestershire, UK) and Falcon (Runcorn, Cheshire, UK). All other reagents were from Sigma-Aldrich (Poole, UK) unless otherwise stated.

Culture of primary BMDM

BMDM were prepared from FVB/nj mice as previously described.[42] Bone marrow was isolated from femurs using aseptic technique and cultured for 7 days in teflon-coated pots in Dulbecco's modified Eagle's medium/F12 with 10% heat-inactivated fetal calf serum, penicillin (100 U/ml), streptomycin (100 μg/ml) and 20% L929 cell-conditioned medium containing macrophage colony-stimulating factor. Mϕ differentiation was confirmed by staining with F4/80-PerCP and CD11b-FITC antibodies (both BD Biosciences, Oxford, UK) before analysis by flow cytometry (Supplementary Figure S5 online). Cytospins were prepared, fixed with ice-cold methanol and stained for HO-1 as described below.

In vitro cytokine and nitrite measurements

BMDM (5×10^5) were plated in 12-well plates and stimulated with lipopolysaccharide and interferon-γ (100 ng/ml and 10 ng/ml, respectively) for 24 h after 24 h of pretreatment with HA (doses from 10 to 100 μmol/l). Mouse tumor necrosis factor-α in the supernatant

was quantitatively measured by sandwich ELISA (R&D system, Abingdon, UK) in accordance with the protocol provided. Absorbance was read at 450 nm and concentration determined by reference to a standard curve.

Murine model of IRI

Female mice aged either 6–8 weeks old (young) or 1-year-old (old) on the FVB/nj strain background were used from in-house colonies. Both age groups were confirmed to be menstruating by measurement of gonadotrophin levels. Procedures were performed under Home Office licences 60/3340 and 60/10547. Anesthesia was induced using Ketamine and Metatomidine via the intraperitoneal route, with Buprenorphine analgesia subcutaneously. By a midline laparotomy a right nephrectomy was performed and the left renal pedicle identified and clipped using an atraumatic clamp for 20 min. During the ischemic period, body temperature was maintained using a heating blanket with homeostatic control (Harvard Apparatus, Boston MA) via a rectal temperature probe. The clamp was then removed, the peritoneum closed with 5/0 suture and the skin closed with clips, and anesthesia reversed using atipamazole. One ml sterile saline was administered subcutaneously before and after surgery. The animals were maintained in an incubator overnight, with further subcutaneous administration of saline given the next morning. Blood and tissue samples were obtained at the time of surgery (d0) and 24 h post-surgery (d1) under terminal anesthesia.

Induction of HO-1 protein

Heme arginate (Orphan Europe, Paris, France) was administered intravenously to selected animals at a dose of 30 mg/kg 24 h before induction of IRI (equating *in vivo* to 38 μmol/l). Paired control animals received equal volumes of PBS. To induce HO-1 in BMDM cultures, cells were cultured for 24 h with 10 μM HA.

Conditional macrophage ablation

For experiments examining ablation of Mϕ, CD11b-DTR animals (FVB/nj background) expressing the receptor for human DT under the control of the CD11b promoter were used as previously described.[16,17,43] On the basis of the previous work, a dose of 10 ng/g body weight of DT was administered to CD11b-DTR or wild-type controls 24 h before IRI to induce renal Mϕ ablation at the time of surgery.

Collection and staining of whole blood for leukocyte populations

Animals were restrained and 25 μl of whole blood was venesected via a tail vein nick. To ensure consistent sample volumes, 25 μl blood was collected from the tail nick using a pipette that already held 25 μl 4.5% citrate solution, resulting in immediate anticoagulation of the collected blood. Samples were stained with CD11b-FITC and Gr1-PE fluorescence-activated cell sorter antibodies, before red cell lysis was performed using BD FACSLyse solution (BD Biosciences) and sample aquisition on a BD FACSCaliber flow cytometer. Analysis was performed using FlowJo software (Treestar, Ashland, OR).

Assessment of renal function

Creatinine concentration in urine and plasma samples was analyzed by the Jaffe method (Alpha Laboratories, Eastleigh, UK) on a Cobas Fara Centrifugal Analyser (Roche Diagnostics, Welwyn Garden City, UK) according to the manufacturer's instructions. Mouse urine albumin levels were measured by a commercial immunoturbidimetric kit (Olympus UK, Watford, UK) adapted for use on the Cobas Fara. The assay was standardized against purified mouse albumin standards.

Western blotting of HO-1 protein

Renal tissue samples were homogenized in lysis buffer (20 mmol/l Tris-HCl, 1 mmol/l EDTA (pH 8.0), 150 mmol/l NaCl and 1% (v/v) Triton-X) supplemented with commercially available antiprotease tablets (Amersham Biosciences, Little Chalfont, UK) and spun at 18,000 *g* for 15 min, after which the liquid phase was mixed with equal volumes of 2 × laemmli buffer (4% SDS, 20% glycerol, 10% 2-mercaptoethanol, 0.004% bromphenol blue, and 0.125 mol/l Tris-HCl) before heating to 95 °C for 5 min. Protein concentrations from *in vivo* homogenates or *in vitro* cell lysates were estimated by the Bio-Rad protein assay reagent (Bio-Rad Laboratories, Hercules, CA). Western Blotting was performed as previously described.[44] Following electrophoresis onto Hybond-P membranes (Amersham, Arlington Heights, IL), the membranes were blocked with 5% dried milk, then incubated overnight at 4 °C with polyclonal rabbit anti-rat antibody (1:5000 dilution; Stressgen Biotechnologies, Vancouver, Canada). After washing in Tris-buffered saline with 0.1% Tween, the blots were incubated with secondary antibody (horseradish peroxidase-conjugated goat anti-rabbit, Sigma) for 1 h. Blots were visualized using the ECL Plus system (Amersham Biosciences). Protein loading was confirmed by reprobing the membranes with anti-β-actin antibody (Sigma, Poole, UK). Densitometric analysis of the images was performed using ImageJ software (ImageJ 1.36b; National Institutes of Health, Bethesda, MD).

Immunohistochemistry

Whole kidneys were cut longitudinally and either snap-frozen in liquid nitrogen or fixed in methyl carnoy's solution (60% methanol, 30% chloroform, and 10% acetic acid) or 4% paraformaldehyde before embedding in paraffin. Four μm tissue sections were cut and stained with hematoxylin and eosin for assessment of medullary acute tubular necrosis, and Picrosirius red for assessment of fibrillar collagen.

For endothelial staining, paraformaldehyde-fixed sections received proteinase K antigen retrieval before staining with Rabbit anti-CD31 Ab (1:100 dilution; BD Pharmingen). Embedded tissue was deparaffinized in xylene, rehydrated and blocked using 3% H_20_2 before incubation with rat anti-F4/80 monoclonal antibody (1/250 dilution; Caltag Laboratories, Northampton, UK) for Renal Mϕ quantification. Infiltrating neutrophils were identified by nuclear morphology combined with immunostaining for the Gr1 (Ly6c/g) antigen using Rat anti-Gr1 monoclonal antibody (1/250 dilution; Cambridge BioScience, Cambridge, UK). Tissue localization of HO-1 was determined following staining with rabbit anti-mouse HO-1 (1/250 dilution; Cambridge BioScience). Primary antibodies were incubated at 4 °C overnight with subsequent incubation with species-specific biotinylated secondary antibody (rabbit anti-rat immunoglobulin-G or goat anti-rabbit immunoglobulin-G, both 1/300 dilution; Vector Laboratories, Peterborough, UK) at room temperature for 30 min. After washing, sections were incubated with Vectastain ABC Elite reagent (Vector Laboratories, Peterborough, UK) for 30 min at room temperature, before washing and staining with diaminobenzidine (Dako UK, Cambridgeshire, UK). Counterstaining was performed with hematoxylin before dehydration and mounting. In all cases, appropriate isotype antibodies were used as negative controls. Mϕ and neutrophils were identified by

morphology and staining pattern, and expressed as mean cells per $\times 400$ microscope field, with five fields being assessed per section. Tubules within the outer stripe of the outer medulla were photographed and tubules were counted as viable or necrotic based on nuclear morphology and the integrity of the epithelial cell layer using ImageJ software (Cell counter plugin; ImageJ 1.36 b; National Institutes of Health, Bethesda, MD). CD31 and Picrosirius red staining was quantified on images acquired $\times 200$ as above, with subsequent analysis of positive staining performed using Colour Range tool on Photoshop CS3 Extended (Version 10.0.1; Adobe Systems Europe, Uxbridge, UK). Results were expressed as a proportion of image pixels positive for CD31 or Picrosirius red.

Immunofluorescence

Frozen tissue was embedded in 22-oxacalcitriol mounting media and 5 μm sections cut, air-dried and fixed in ice-cold acetone. For *in vitro* preparations, cytospins were prepared as described above. After protein blockade (Spring Bioscience, Pleasanton, CA) primary antibodies (polyclonal rabbit anti-HO-1, rat anti-mouse CD68) were added at 1:250 dilution and incubated for 1 h at room temperature. Following washing in PBS, secondary antibodies (Alexa-568-conjugated goat anti-rabbit immunoglobulin and Alexa-488 donkey anti-rat immunoglobulin-, both from Invitrogen, Paisley, UK) were added at 1:500 dilution for 1 h. Slides were coverslipped with Vectashield-containing DAPI (Vector Laboratories) before microscopy and image aquisition. Image analysis was performed as previously described using Photoshop CS3.

Statistical analysis

All data are expressed as mean ± s.e.m. The Student's unpaired *t*-test was used to compare two groups. Where multiple conditions were compared, the one-way analysis of variance for repeated measurements was used. *P*-values <0.05 were taken as representing statistical significance. All statistical analysis was performed using GraphPad Prism version 4.0c for Macintosh (GraphPad Software, San Diego, CA, www.graphpad.com).

DISCLOSURE

All the authors declared no competing interests.

ACKNOWLEDGMENTS

We thank Dr Forbes Howie for his assistance with creatinine measurements and Bob Morris and Susan Harvey for their excellent work in the preparation of histological sections. This work was supported by MRC Grant G0801235 to JH and DCK, and the award to DAF of fellowships from Kidney Research UK, Medical Research Scotland and funds from the Kerr-Fry and Urquhart bequests. NCJN was funded by the Royal Infirmary of Edinburgh Renal Endowment Fund. DCK was the recipient of a Kidney Research UK project grant. This work was also funded by Kidney Research UK Grant TF17/2005, Medical Research Scotland Grant FRG243 to DAF, and Lothian Renal Endowment Fund 07187 to NCJN.

SUPPLEMENTARY MATERIAL

Figure S1. Identification of the renal microvaculature using immunohistochemistry for the CD31 antigen.
Figure S2. Typical immunohistochemical appearances of cortex and medulla of young and old kidneys (A).
Figure S3. FACS analysis of whole blood before and after HA administration (or PBS control) demonstrates no alteration in total leukocyte counts at 1 day after injection (A).
Figure S4. Western blotting of protein homogenate from bone marrow-derived macrophages, demonstrates progressive induction of HO-1 up to 24h of exposure to heme arginate, which was maintained for up to 48 h after removal of HA containing media (A).
Figure S5. Bone marrow-derived macrophages co-express high levels of the classical macrophage markers CD11b and F4/80 by flow cytometry after 7 days culture *in vitro*.
Table S1. Summary of tubular necrosis scores, hemeoxygenase protein levels and leukocyte counts in young and old mice after ischaemia-reperfusion injury.
Supplementary material is linked to the online version of the paper at http://www.nature.com/ki

REFERENCES

1. Thadhani R, Pascual M, Bonventre JV. Acute renal failure. *N Engl J Med* 1996; **334**: 1448–1460.
2. Xue JL, Daniels F, Star RA *et al.* Incidence and mortality of acute renal failure in Medicare beneficiaries, 1992 to 2001. *J Am Soc Nephrol* 2006; **17**: 1135–1142.
3. Ishani A, Xue JL, Himmelfarb J *et al.* Acute kidney injury increases risk of ESRD among elderly. *J Am Soc Nephrol* 2009; **20**: 223–228.
4. Schmitt R, Coca S, Kanbay M *et al.* Recovery of kidney function after acute kidney injury in the elderly: a systematic review and meta-analysis. *Am J Kidney Dis* 2008; **52**: 262–271.
5. Schmitt R, Cantley LG. The impact of aging on kidney repair. *Am J Physiol Renal Physiol* 2008; **294**: F1265–F1272.
6. Wagener FA, Volk HD, Willis D *et al.* Different faces of the heme-heme oxygenase system in inflammation. *Pharmacol Rev* 2003; **55**: 551–571.
7. Maines MD, Mayer RD, Ewing JF *et al.* Induction of kidney heme oxygenase-1 (HSP32) mRNA and protein by ischemia/reperfusion: possible role of heme as both promotor of tissue damage and regulator of HSP32. *J Pharmacol Exp Ther* 1993; **264**: 457–462.
8. Nath KA. Heme oxygenase-1: a provenance for cytoprotective pathways in the kidney and other tissues. *Kidney Int* 2006; **70**: 432–443.
9. Tzima S, Victoratos P, Kranidioti K *et al.* Myeloid heme oxygenase-1 regulates innate immunity and autoimmunity by modulating IFN-beta production. *J Exp Med* 2009; **206**: 1167–1179.
10. Roach JP, Moore EE, Partrick DA *et al.* Heme oxygenase-1 induction in macrophages by a hemoglobin-based oxygen carrier reduces endotoxin-stimulated cytokine secretion. *Shock* 2009; **31**: 251–257.
11. Gueler F, Park JK, Rong S *et al.* Statins attenuate ischemia-reperfusion injury by inducing heme oxygenase-1 in infiltrating macrophages. *Am J Pathol* 2007; **170**: 1192–1199.
12. Devey L, Ferenbach D, Mohr E *et al.* Tissue-resident macrophages protect the liver from ischemia reperfusion injury via a heme oxygenase-1-dependent mechanism. *Mol Ther* 2009; **17**: 65–72.
13. Bloomer SA, Zhang HJ, Brown KE *et al.* Differential regulation of hepatic heme oxygenase-1 protein with aging and heat stress. *J Gerontol A Biol Sci Med Sci* 2009; **64**: 419–425.
14. Ewing JF, Maines MD. Regulation and expression of heme oxygenase enzymes in aged-rat brain: age related depression in HO-1 and HO-2 expression and altered stress-response. *J Neural Transm* 2006; **113**: 439–454.
15. Ito Y, Betsuyaku T, Moriyama C *et al.* Aging affects lipopolysaccharide-induced upregulation of heme oxygenase-1 in the lungs and alveolar macrophages. *Biogerontology* 2009; **10**: 173–180.
16. Henderson NC, Mackinnon AC, Farnworth SL *et al.* Galectin-3 expression and secretion links macrophages to the promotion of renal fibrosis. *Am J Pathol* 2008; **172**: 288–298.
17. Duffield JS, Tipping PG, Kipari T *et al.* Conditional ablation of macrophages halts progression of crescentic glomerulonephritis. *Am J Pathol* 2005; **167**: 1207–1219.
18. Thomas SE, Anderson S, Gordon KL *et al.* Tubulointerstitial disease in aging: evidence for underlying peritubular capillary damage, a potential role for renal ischemia. *J Am Soc Nephrol* 1998; **9**: 231–242.
19. Vercauteren SR, Ysebaert DK, De Greef KE *et al.* Chronic reduction in renal mass in the rat attenuates ischemia/reperfusion injury and does not impair tubular regeneration. *J Am Soc Nephrol* 1999; **10**: 2551–2561.
20. Mahler JF, Stokes W, Mann PC *et al.* Spontaneous lesions in aging FVB/N mice. *Toxicol Pathol* 1996; **24**: 710–716.
21. Sabbatini M, Sansone G, Uccello F *et al.* Functional versus structural changes in the pathophysiology of acute ischemic renal failure in aging rats. *Kidney Int* 1994; **45**: 1355–1361.

22. Moore BA, Albers KM, Davis BM *et al.* Altered inflammatory gene expression underlies increased susceptibility to murine postoperative ileus with advancing age. *Am J Physiol Gastrointest Liver Physiol* 2007; **292**: G1650–G1659.
23. Exner M, Minar E, Wagner O *et al.* The role of heme oxygenase-1 promoter polymorphisms in human disease. *Free Radic Biol Med* 2004; **37**: 1097–1104.
24. Leonard MO, Kieran NE, Howell K *et al.* Reoxygenation-specific activation of the antioxidant transcription factor Nrf2 mediates cytoprotective gene expression in ischemia-reperfusion injury. *FASEB J* 2006; **20**: 2624–2626.
25. Liu M, Grigoryev DN, Crow MT *et al.* Transcription factor Nrf2 is protective during ischemic and nephrotoxic acute kidney injury in mice. *Kidney Int* 2009.
26. Yoon HY, Kang NI, Lee HK *et al.* Sulforaphane protects kidneys against ischemia-reperfusion injury through induction of the Nrf2-dependent phase 2 enzyme. *Biochem Pharmacol* 2008; **75**: 2214–2223.
27. Duan W, Zhang R, Guo Y *et al.* Nrf2 activity is lost in the spinal cord and its astrocytes of aged mice. *In Vitro Cell Dev Biol Anim* 2009; **45**: 388–397.
28. Jadhav A, Ndisang JF. Heme arginate suppresses cardiac lesions and hypertrophy in deoxycorticosterone acetate-salt hypertension. *Exp Biol Med (Maywood)* 2009; **234**: 764–778.
29. Jadhav A, Torlakovic E, Ndisang JF. Hemin therapy attenuates kidney injury in deoxycorticosterone acetate-salt hypertensive rats. *Am J Physiol Renal Physiol* 2009; **296**: F521–F534.
30. Wilson HM, Chettibi S, Jobin C *et al.* Inhibition of macrophage nuclear factor-kappaB leads to a dominant anti-inflammatory phenotype that attenuates glomerular inflammation *in vivo*. *Am J Pathol* 2005; **167**: 27–37.
31. Shimizu H, Takahashi T, Suzuki T *et al.* Protective effect of heme oxygenase induction in ischemic acute renal failure. *Crit Care Med* 2000; **28**: 809–817.
32. Ollinger R, Kogler P, Biebl M *et al.* Protein levels of heme oxygenase-1 during reperfusion in human kidney transplants with delayed graft function. *Clin Transplant* 2008; **22**: 418–423.
33. Holzen JP, August C, Bahde R *et al.* Influence of heme oxygenase-1 on microcirculation after kidney transplantation. *J Surg Res* 2008; **148**: 126–135.
34. da Silva JL, Zand BA, Yang LM *et al.* Heme oxygenase isoform-specific expression and distribution in the rat kidney. *Kidney Int* 2001; **59**: 1448–1457.
35. Day YJ, Huang L, Ye H *et al.* Renal ischemia-reperfusion injury and adenosine 2A receptor-mediated tissue protection: role of macrophages. *Am J Physiol Renal Physiol* 2005; **288**: F722–F731.
36. Jo SK, Sung SA, Cho WY *et al.* Macrophages contribute to the initiation of ischaemic acute renal failure in rats. *Nephrol Dial Transplant* 2006; **21**: 1231–1239.
37. Rae F, Woods K, Sasmono T *et al.* Characterisation and trophic functions of murine embryonic macrophages based upon the use of a Csf1r-EGFP transgene reporter. *Dev Biol* 2007; **308**: 232–246.
38. Ferenbach D, Hughes J. Macrophages and dendritic cells: what is the difference? *Kidney Int* 2008; **74**: 5–7.
39. Soos TJ, Sims TN, Barisoni L *et al.* CX3CR1+ interstitial dendritic cells form a contiguous network throughout the entire kidney. *Kidney Int* 2006; **70**: 591–596.
40. Kubulus D, Mathes A, Pradarutti S *et al.* Hemin arginate-induced heme oxygenase 1 expression improves liver microcirculation and mediates an anti-inflammatory cytokine response after hemorrhagic shock. *Shock* 2008; **29**: 583–590.
41. Ferenbach DA, Ramdas V, Spencer N *et al.* Macrophages expressing heme oxygenase-1 improve renal function in ischemia reperfusion injury. *Mol Ther* 2010; **18**: 1706–1713.
42. Duffield JS, Erwig LP, Wei X *et al.* Activated macrophages direct apoptosis and suppress mitosis of mesangial cells. *J Immunol* 2000; **164**: 2110–2119.
43. Cailhier JF, Partolina M, Vuthoori S *et al.* Conditional macrophage ablation demonstrates that resident macrophages initiate acute peritoneal inflammation. *J Immunol* 2005; **174**: 2336–2342.
44. Datta PK, Koukouritaki SB, Hopp KA *et al.* Heme oxygenase-1 induction attenuates inducible nitric oxide synthase expression and proteinuria in glomerulonephritis. *J Am Soc Nephrol* 1999; **10**: 2540–2550.